CrossMark

Thermal properties, nanoscopic structure and swelling behavior of chitosan/(ureasil–polyethylene oxide hybrid) blends

Mayté Paredes Zaldivar[1,2] · Celso Valentim Santilli[1] · Carlos Andrés Peniche Covas[3] · Sandra Helena Pulcinelli[1]

Abstract In this work, the effect of chitosan blending on the thermal properties, nanoscopic structure and swelling behavior of ureasil–polyethylene oxide (U-PEO) hybrid materials was examined. Materials were prepared by the sol–gel route using acid catalysts, and the effect of acid (hydrochloric or acetic acid) was also examined. Differential scanning calorimetry results showed that chitosan addition did not provoke appreciable changes in the thermal behavior of the U-PEO. Thermogravimetric curves did not show changes in thermal stability resulting from chitosan blending but were depended on the type of acid catalyst. Small-angle X-ray scattering and nuclear magnetic resonance spectroscopy techniques were used for studying nanoscopic and inner structures, showing the existence of two structural levels and differences in polycondensation degrees. All samples presented fast water uptake with the same initial swelling rate and with a non-Fickian or anomalous transport mechanism. Swelling degree was higher in hybrids prepared with HCl, which possessed less branched siloxane cross-link nodes species, therefore lower polycondensation degree. Also, the magnitude of swelling decreased for hybrids blended with chitosan, which provides a means of tailoring the water uptake by the ureasil–PEO hybrid and to potentiate the control of the release profile of drugs incorporated in these materials.

Introduction

Siloxane-polyether hybrids, also named ureasils, are an interesting and versatile family of multifunctional organic–inorganic hybrid (OIH) materials. They are composed of a siloxane backbone covalently connected to polyether chains of variable length by means of urea bridges [1, 2]. These hybrids are biocompatible, transparent, rubbery, flexible and insoluble in water [1]. Ureasils have been the object of intensive studies in the last years due to their wide range of applications. They can be used as solid-state electrochromic devices, tunable photo-luminescent materials, ionic conductors, adsorbents for environmental applications and drug delivery systems [3–5].

Polyethylene oxide (PEO) is commonly used as polyether chain in the synthesis of these hybrids [2, 3, 6]. It is one of the most important synthetic polymers used in the pharmaceutical industries due to its biocompatibility, non-toxicity and high water-solubility and swellability [7]. Their hydrophilic nature inhibits protein adsorption, cell adhesion and provides its own full excretion. PEO can be used also in block copolymers or in cross-linked networks [8].

Previously, we reported the synthesis of a new OIH material, the chitosan/(ureasil–polyethylene oxide hybrid) blend [6]. Chitosan is a biodegradable, biocompatible and low toxicity polymer with numerous biological properties [9]. The blend and the hybrid without chitosan were prepared by the sol–gel route, using hydrochloric acid (HCl)

✉ Mayté Paredes Zaldivar
mayte.paredeszaldivar@gmail.com

1 Instituto de Química, Universidade Estadual Paulista (UNESP), São Paulo, Brazil

2 Centro de Aplicaciones Tecnológicas y Desarrollo Nuclear (CEADEN), Habana, Cuba

3 Centro de Biomateriales (BIOMAT), Universidad de La Habana, Habana, Cuba

as catalyst, and were loaded with pramoxine hydrochloride, as a model drug. The systemic study showed that the combined addition of chitosan and pramoxine improved the compatibility of the organic and inorganic components of the matrix, and provided a means of tailoring the amount of drug released [6].

Chitosan is a pH-sensitive natural cationic polymer that remains insoluble in neutral aqueous environment but becomes soluble in acid media due to the protonation of its amino groups [9]. It is well known that acetic acid (HAc) is commonly used to dissolve chitosan [10]; therefore, in our research similar hybrids materials were obtained with HAc as acid catalyst. In this work, we report the effect of chitosan blending on the thermal properties, nanoscopic structure and swelling behavior of Ureasil–PEO (U-PEO) hybrid materials. The effect of the type of acid, HCl or HAc, used as catalyst in the hydrolytic sol–gel synthesis was also studied.

Experimental

Synthesis of the hybrid materials

A well-known synthesis procedure was adopted for the hybrid precursor preparation [6, 8] involving the reaction of terminal aminopropyl groups of the functionalized PEO macromer (O,O′-bis-(2-aminopropyl) polypropylene glycol-block-polyethylene glycol-block-polypropylene glycol 1900, Fluka) with 3-(isocyanatopropyl)-triethoxysilane (Aldrich), using a molar ratio of 1:2. The reagents were stirred together in tetrahydrofuran (THF) under reflux for 24 h. Following this, THF was eliminated by evaporation at 60 °C, producing the hybrid precursor. In the second step, silanol moieties were generated, followed by condensation reactions to form ureasil cross-linking nodes [1]. The hydrolysis of $Si(OCH_2CH_3)_3$ was initiated by adding an ethanol(eth)/water(H_2O) mixture (0.03 v/v) containing acid catalyst (HCl or HAc, 2 M) to the precursor. For the blend, 3 mass% of chitosan (CHI, 57,000 g mol^{-1}, DD = 88%, Sigma-Aldrich) dissolved in the acid hydrolysis solution were incorporated into the hybrid precursor, as shown in Table 1. Monolithic U-PEO and U-PEO/CHI xerogels were obtained after drying under vacuum at room

temperature for 7 days [6]. During drying at room temperature only the solvents, ethanol and water, are lost, so all the added chitosan remains in the xerogel. All reagents were used without purification, except chitosan, that was purified by dissolution in dilute aqueous acetic acid followed by precipitation with NaOH (1 M), as described in our previous work [6].

Characterization

Thermal properties of hybrids were assessed by differential scanning calorimetry, DSC, (TA Instruments Model DSC Q100 analyzer) and thermogravimetric analysis, TG, (Q600 SDT TA Instruments). The thermal events were investigated at a heating rate of 10 °C min^{-1} and monitoring between −90 and 350 °C and 25–600 °C for DSC and TG, respectively. All analyzes were performed under nitrogen flow (50 cm^3 min^{-1} for DSC and 100 cm^3 min^{-1} for TG) and between 5 mg and 10 mg of sample were used in measurements.

The nanostructures of the U-PEO and U-PEO/CHI hybrids were evaluated by small-angle X-ray scattering, SAXS, measurements carried out at 25 °C at the SAXS1 beamline of the National Synchrotron Light Laboratory (LNLS, Campinas, Brazil). The beamline was equipped with an asymmetrically cut and bent silicon (111) monochromator that produced a focused monochromatic beam ($\lambda = 0.1550$ nm). A bi-dimensional photon counting pixel detector (Pilatus 300 k) was used to record the scattering intensity, $I(q)$, as a function of the modulus of the scattering vector $q = (4\pi/\lambda) \sin(\theta)$ (2θ = scattering angle), resulting in a q-range span of 0.12–4.10 nm^{-1}. A pin diode inserted in the 6 mm beam stop was used to record the transmitted intensity in order to correct the natural beam intensity decay. SAXS patterns were recorded for dried samples.

The chemical environment of silicon atoms of the siloxane nodes was analyzed by solid-state nuclear magnetic resonance spectroscopy, ^{29}Si MAS-NMR, measurements carried out with an INOVA 300 Varian spectrometer at the Larmor frequency of 59.59 MHz and field of 7.05 T. The following parameters were fixed for ^{29}Si: spectral width of 62.5 kHz; pulse of 90° (5.5 μs); relaxation time of

Table 1 Experimental conditions for hybrid synthesis

	M (prec)/g	M (CHI)/g	V (H_2O)/μL	V (eth)/μL	V (acid)/μL
U-POE (HCl)	0.7500	–	1500	50	17.5 (HCl)
U-POE (HAc)	0.7500	–	1500	50	17.5 (HAc)
U-POE/CHI (HCl)	0.7500	0.0232	1500	50	17.5 (HCl)
U-POE/CHI (HAc)	0.7500	0.0232	1500	50	17.5 (HAc)

200 s and rotation of 5.5 kHz. Chemical shifts were relative to tetramethylsilane (TMS), used as external standard. Proton decoupling was always used during acquisition of the spectra. Due to the high sensitivity of the ^{29}Si NMR measurements, the uncertainty in the chemical shift values was less than 0.2 ppm.

To determine the dynamic swelling behavior caused by water uptake, pre-weighed dry hybrid disks were immersed in distilled water at 25 °C. The disks were taken out of the water and weighed at specified time intervals after excessive surface water was blotted. The swelling percentage caused by the water uptake, S, was calculated as:

$$S = \frac{(M_t - M_0)}{M_0} * 100 \, (\%) \tag{1}$$

where M_t is the mass of sample after the water absorption at time t and M_0 is the mass of the dry sample [11].

In order to study the swelling mechanism, the empirical power law relationship proposed by Ritger and Peppas [11–13] was considered to describe the experimental time evolution:

$$\frac{M_t}{M_\infty} = k t^n \tag{2}$$

where M_∞ is the mass of water absorbed at equilibrium, k is a constant and the exponent n is function of the water uptake transport mechanism. This empirical model is accurate only for the early portion of the water absorption curve ($M_t/M_\infty \leq 0.60$).

Results and discussion

Thermal behavior

DSC curves of ureasil–PEO generally show two characteristic events: the deviation from the baseline (between −60 and −30 °C) associated with the glass transition temperature (T_g) and one endothermic peak (around 30 °C) characteristic of the melting of semi-crystalline PEO (T_m) [1]. Figure 1a shows these events for the U-PEO and U-PEO/CHI hybrids. The glass transition temperatures (Fig. 1b) did not show significant changes neither by chitosan addition nor by the type of acid, suggesting that the PEO chain mobility and inter-chain interactions of the amorphous polymer phase were not affected by these parameters.

The DSC curve of pristine chitosan is also presented in Fig. 1a. It is characterized by the glass transition at 52 °C and two peaks corresponding to dehydration (120 °C) and decomposition (285 °C) processes of this polymer [14], respectively. The start of the chitosan decomposition process could be seen for the hybrid prepared with HCl, but it

is absent for the hybrid prepared with HAc. This fact could be explained by a partial and total dissolution of chitosan in the hybrid matrix prepared in the presence of HCl and HAc solution, respectively.

The crystallinity degree (CD) of these hybrids was calculated as the ratio between the experimental melting enthalpies per gram of PEO (ΔH_m) and the melting enthalpy per gram of 100% crystalline PEO ($\Delta H_m = 196.4 \, \text{J g}^{-1}$) [15]. These parameters are presented in Table 2. The calculated CD values and the melting temperatures do not have significant differences, indicating that the studied parameters do not modify the natural crystallization tendency of PEO in the hybrid matrix.

Thermal stability of U-PEO and U-PEO/CHI was studied by thermogravimetry, by measuring the mass loss as a function of temperature. The TG and derivative TG (DTG) curves of hybrids and chitosan are displayed in Fig. 2a. All curves show an initial mass loss below 120 °C, which can be attributed to the release of adsorbed molecules (water and ethanol) [16, 17]. The chitosan curve shows another degradation stage, corresponding to the main decomposition of this polymer, generating a carbonaceous material. The decomposition is associated with the rupture of polysaccharide chains by dehydration, deamination, deacetylation, breaking of glycoside bonds and pyranose ring opening [14, 16, 18, 19]. The temperature of maximum decomposition rate (T_{max}) occurs at 275 °C. This main decomposition stage is observed in the U-PEO/CHI (HCl) hybrid, evidencing the partial and total dissolution of chitosan in the hybrids prepared with HCl and HAc solutions, respectively (Fig. 2b).

The main degradation stage of the hybrid materials starts at about 310 °C and could be attributed to ureasils decomposition [17]. The DTG trace evidence that the samples can be classed by two set of temperature of maximum decomposition rates. These temperature values do not change by chitosan addition and depend only on the type of acid used as catalyst. T_{max} of hybrids prepared with HCl (404 °C) is higher than that of hybrids prepared with HAc (390 °C), indicating that the first ones are thermally more stable. One possible explanation for this result could be the formation of more compact siloxane aggregates dispersed in the matrix for hybrids made with HCl, that need more energy for their decomposition.

Siloxane species and Nanostruture

The effect of the chitosan blending and the acid catalyst on the condensation degree and the inner structure of siloxanes of the organic–inorganic hybrid materials were studied by ^{29}Si NMR. Figure 3 displays the NMR spectra with each resonance identified by the conventional notation T_y^x,
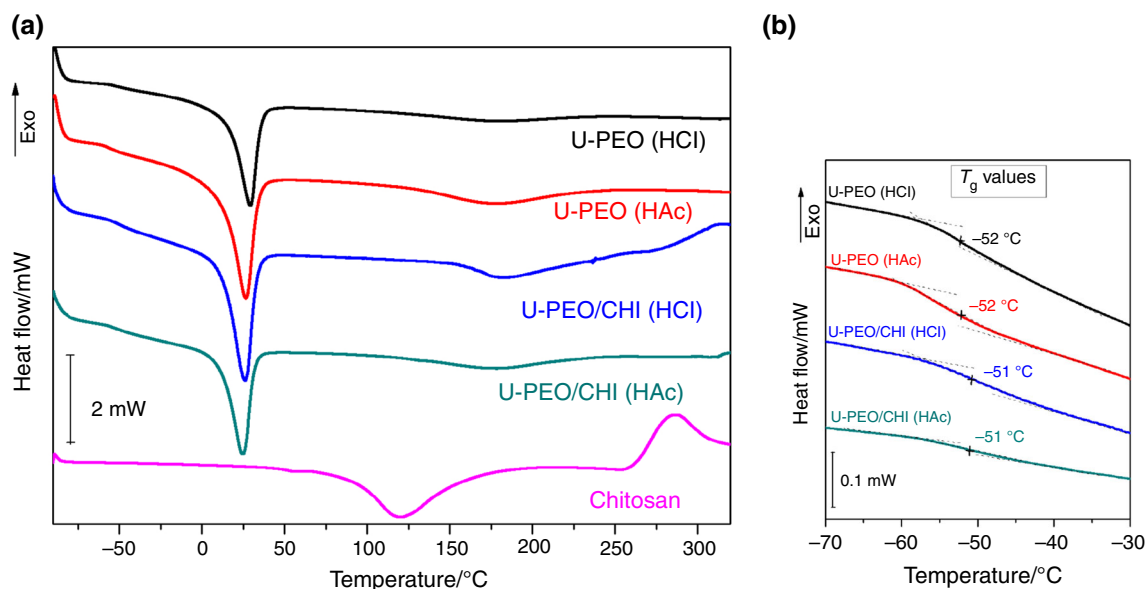
Fig. 1 DSC heating curves; **a** for the U-PEO and U-PEO/CHI hybrid materials prepared with different acid catalyst and for pristine chitosan, and **b** enlarged curve plots for the low temperature region, showing the glass transition event

Table 2 Values of melting temperatures, melting enthalpies and crystallinity degrees of hybrid materials

	Tm_{onset}/°C	ΔH_m/J g^{-1}	CD/%
U-POE (HCl)	15	39	20
U-POE (HAc)	14	36	18
U-POE/CHI (HCl)	12	34	17
U-POE/CHI (HAc)	13	34	17

$(RSi(OSi)_x(OH)_{3-x})_y$. The superscript x denotes the number of siloxane bonds and the subscript y denotes the number of trifunctional units composing each distinct structure. The ^{29}Si NMR spectrum corresponding to U-PEO prepared under HCl catalysis display four main resonances, evidencing the coexistence of uncondensed T^o units, $RSi(OH)_3$ ($\delta = -42.0$ ppm), dimer T^1 $RSi(OSi)$ $(OH)_2$ ($\delta = -50.0$ ppm) as a shoulder, linear T^2 or cyclic T_3^2 $(RSi(OSi)_2(OH)_1)_3$ ($\delta = -54.6$ and -55.9 ppm)
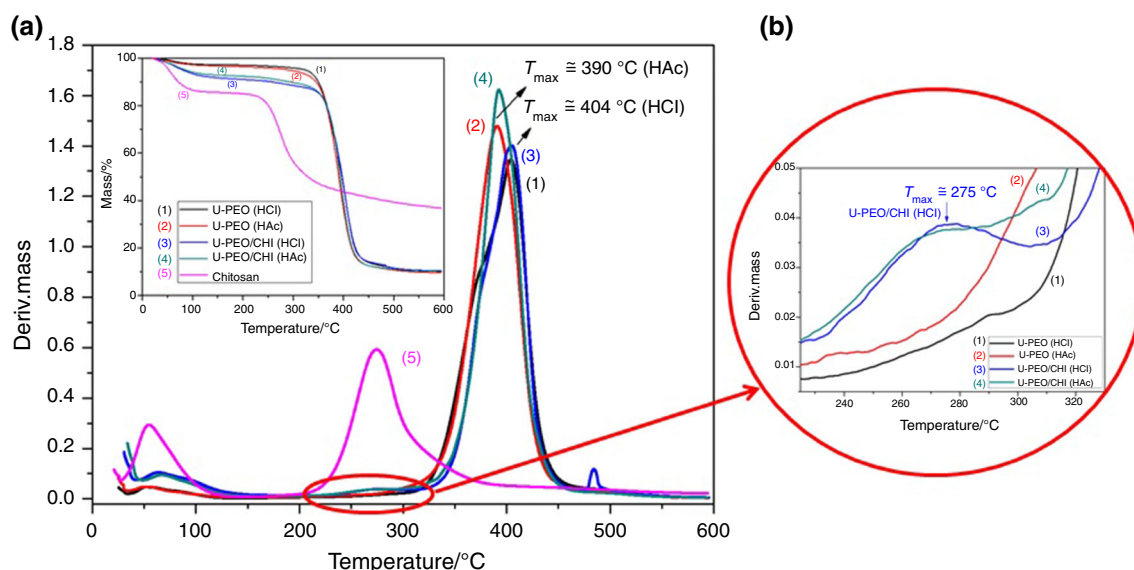

Fig. 2 Thermal analysis; **a** TG (*insert*) and DTG curves for the U-PEO and U-PEO/CHI hybrid materials prepared with different acid catalyst and for pristine chitosan, and **b** enlarged curve plots in the chitosan decomposition region
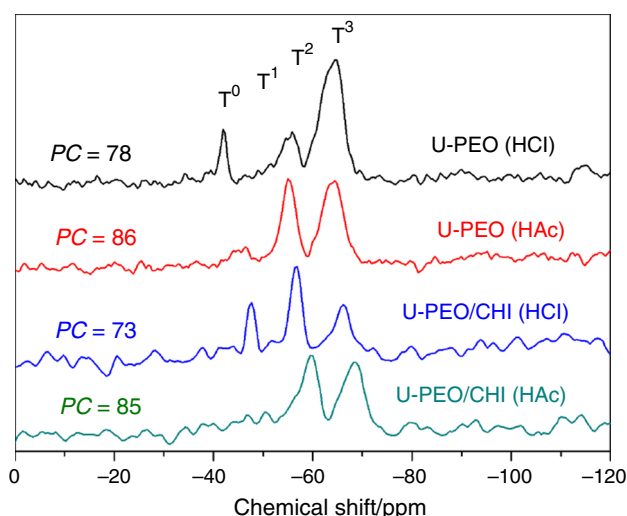
Fig. 3 ^{29}Si MAS-NMR spectra of U-PEO and U-PEO/CHI hybrids prepared under HCl and HAc catalyst

species and fully condensed strained hexahedral structure T_6^3 $(RSi(OSi)_3)_6$ ($\delta = -64.4$ ppm) [20–22]. The presence of monomeric species (T^0 units) in the mixture with dimeric (T^1) and polyhedral (T^2 and T^3) species suggests that the formation of condensed species occurs by a monomer-cluster growth mechanism [23].

For U-PEO prepared under HAc catalysis, the resonance of uncondensed T^0 units disappear and the T^2 band become narrow and as intense as the T^3 one. The equivalent intensity observed for T^2 and T^3 bands is expected for disilanol $T_8(OH)_2$ $(R_8Si_8O_{11}(OH)_2)$ structures [24–27]. These features evidence the higher efficiency of polycondensation reaction as compared with hybrid prepared under HCl catalyst. In fact, the absence of monomeric species indicates that the formation of condensed species occurs by reaction limited cluster–cluster growth which is expected when the rate of condensation reactions is higher than the rate of hydrolysis, leading to the fast consumption of all monomeric species [23].

The chitosan blending affects significantly the inner structure of siloxanes. For hybrid blend prepared under HCl catalyst, the spectra is dominated by the intense peak at -56.3 ppm which possibly originates from the T^2 silicon of the more strained three-membered ring in hexahedron. However, the coexistence of this band with the T^3 resonance at -66.2 ppm and the terminal T^1 units at -47.6 suggests also the presence of trisilanol $T_7(OH)_3$ [24–27]. The U-PEO/CHI prepared under HAc display an equivalent shift of the T^2($\Delta\delta = 4.6$ ppm) and T^3($\Delta\delta = 4.1$ ppm) as compared to U-PEO resonances, suggesting that the chitosan blending induces the increase in the hydroxylation degree from disilanol $T_8(OH)_2$ to trisilanol $T_7(OH)_3$ octahedron [24, 27].

The polycondensation degree, PC, was calculated from the proportion of each species by measuring the areas of the ^{29}Si resonance peaks and considering the PC value expected for the different T^x units, where PC values are 100, 66.7, 33.3 and 0.0% for T^3, T^2, T^1 and T^0, respectively [2]. These results, presented in Fig. 3, showed that the PC values are higher for hybrids prepared with HAc evidencing that more branched species were obtained. This feature can be explained from the more acid pH of reactional solutions containing HCl (pH = 1.4) as compared with that catalyzed under HAc (pH = 3.1). The last one favors base-catalysed silanol condensation reaction, while under HCl catalyst the pH below the point-of-zero-charge of sílica (pH $\approx$ 2) the hydrolysis reactions are faster, resulting in less branched silicon species [28]. It is also appreciated that chitosan hindered the PC for U-PEO/CHI (HCl) probably due to their partial dissolution in the hybrid matrix prepared with HCl, while the total dissolution of chitosan in the presence of HAc solution allowed condensation reactions to be achieved more easily.

The effect of the chitosan blending and of the acid catalyst nature on the nanoscopic structure of U-PEO hybrid was studied by SAXS and the results were displayed on the double logarithmic plot of Fig. 4. The curves showed the existence of two well-defined regimes suggesting the exitance of two structural levels. The first one was evidenced by the broad peaks located at high q values and the second one by a linear decay in the intensity at low q values. The single peak provides evidence for a strong spatial correlation between the regularly spaced siloxane cross-link nodes present in the first structural level. The average correlation distance between two adjacent siloxane nodes ($d_s \approx 4.1$ nm), calculated using $d_s = 2\pi/q_{max}$, was unaffected by the incorporation of chitosan or by the nature of the used acid.
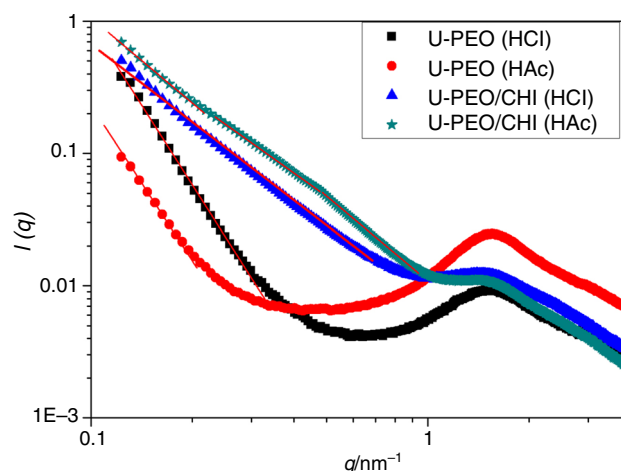

Fig. 4 SAXS curves (log–log plot) of U-PEO and U-PEO/CHI hybrids prepared under HCl and HAc catalyst

The second level was characterized by an asymptotic linear trend in the lower q-range, which satisfies the Porod's law $I(q) \sim q^{-\alpha}$ [29, 30]. The Porod exponent $\alpha \approx 3.6$ verified for U-PEO prepared under HCl and HAc hydrolysis indicates the existence of a biphasic structure, presenting coarse domains with a rough interphase. Probably these domains are formed by the crystalline PEO embedded in a less dense U-PEO matrix. The shift of this linear regime toward lower q-range verified for hybrids prepared with HAc, indicate an increase in size of the crystalline domains [20]. The exponent $\alpha \approx 2$ observed for U-PEO/CHI prepared under HCl hydrolysis points to the scattering from Gaussian polymer chains [23], indicating that chitosan blended in the U-PEO hybrid matrix behave as an ideal chain solution, with neglected volume interactions. On opposition, U-PEO/CHI sample prepared with HAc presented two linear regimes the high-q and the low-q region corresponding to $\alpha \approx 3$ which points to scattering from collapsed polymer chains (in a bad solvent), while the intermediate-q region corresponds to $\alpha \approx 2$ points to scattering from polymer chains in a good solvent [30]. This feature suggests the coexistence of chitosan chain in both swollen and shrunken conformations.

Swelling

Figure 5 presents the dynamic swelling behavior of the OIH immersed in water at 25 °C. All samples showed a rapid water uptake with the same initial rate of swelling. This rate was determined from the slope of the asymptotic linear behavior of the curve at the first 10 min, and the obtained value was 0.12 ± 0.02 g (H_2O) g $(hybrid)^{-1}$ min^{-1}. High degrees of swelling were obtained with water uptake values

between 185 and 300%, showing hydrogel behavior. Hydrogels are hydrophilic polymeric networks capable of absorbing and retaining large amounts of water and/or biological fluids, without losing its three-dimensional shape [31], as highlighted by the picture inserted in Fig. 5. Swelling involves the hydrogel network expansion by water absorption, which results in the increasing of the free volume between the polymeric chains.

When chitosan is added to the hybrid systems the swelling degree decreases, indicating that chitosan reduces the hydrophilicity of these matrices. This reduction is more evident for hybrids prepared with HCl, maybe by the partial dissolution of this polymer in the matrix.

It can be seen that the swelling degrees of hybrids prepared with HCl were higher than those prepared with HAc. This fact could be explained by the differences in the matrix polycondensation degree caused by the pH of the acid used as catalysts in the hydrolysis and condensation reactions of the sol–gel method. The more branched species obtained with HAc hindered the matrix water uptake, while the presence of higher amount of uncondensed silanol species in the OIH prepared with HCl allowed the decrease in the rigidity and the hydrophobic character of the siloxanol nodes, favoring the water uptake.

A mathematical analysis of the swelling behavior was done for elucidating the water transport mechanism involved in the hybrids swelling. The Ritger–Peppas model [11–13] is generally used to analyze the swelling and/or drug release processes when the mechanism is not well understood, or when more than one phenomenon may be involved. Water transport into the hybrid matrix can be attributed to primarily two mechanisms: diffusion and relaxation. This model allows calculating n, the exponent that can describe the mode of the penetrant transport mechanism. For a film, $n = 0.5$ indicates Fickian diffusion, $0.5 < n < 1$ non-Fickian or anomalous transport, and
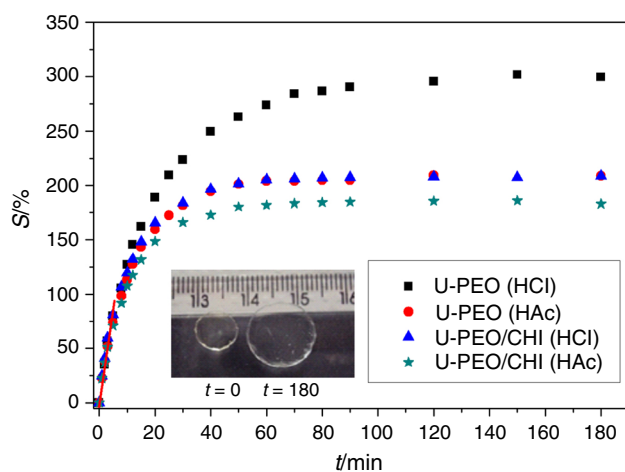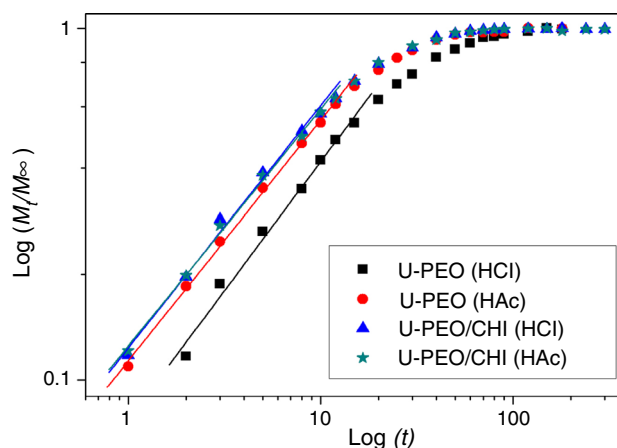

Fig. 5 Swelling percentage (S) as a function of immersion time in water. All values are the average of three readings, with a standard deviation ≤ 3 °C. The *insert* shows the typical variation in shape of the hydrogel after swelling

Fig. 6 Log–log plot of the fractional water uptake (M_t/M_∞) as a function of time. The *solid line* represents the linear regression fit

Table 3 Values of n and k parameters from Eq. (2) at 25 °C (average $\pm$ SD, $N = 3$, $R^2 > 0.99$)

	n	k
U-POE (HCl)	0.73 ($\pm$0.04)	0.08 ($\pm$0.03)
U-POE (HAc)	0.69 ($\pm$0.01)	0.11 ($\pm$0.01)
U-POE/CHI (HCl)	0.69 ($\pm$0.03)	0.12 ($\pm$0.02)
U-POE/CHI (HAc)	0.67 ($\pm$0.02)	0.13 ($\pm$0.01)

$n = 1$ implies case II (relaxation-controlled) transport [11–13, 32].

The water absorption curves (M_t/M_∞ vs. t) for the hybrid materials were plotted in Fig. 6 and fitted to the linearized Ritger–Peppas equation, Eq (2). The calculated constants, n and k, are given in Table 3. Values of n around 0.7 were obtained for all hybrids, indicating that the transport mechanism was non-Fickian or anomalous. This means that swelling occurs by both diffusion and relaxation-controlled mechanisms. Transport is governed, to a large extent, by diffusive fluxes under concentration gradients that exist within the gels, but relaxations can also contribute to this process by the viscoelastic properties of the polymeric phase [33]. These results evidence that neither the addition of chitosan nor the acid used as catalyst had an effect on the swelling mechanism. Also, it can be seen that a remarkably good agreement is obtained between the value of k and the initial swelling rate evaluated from the initial slope of the experimental curve.

Conclusions

This paper demonstrates that the chitosan blending did not essentially affect the thermal properties of ureasil–PEO hybrid materials, i.e., the glass transition and melting temperatures, enthalpies and the degree of crystallization determined from DSC measurements. Otherwise, thermogravimetric results have evidenced that hybrids prepared with HCl were thermally more stable than hybrids prepared with HAc, and that no changes in the thermal stability were found by the presence of the polymer.

The study showed the existence of two nanoscopic structural levels, suggesting a hierarchical structure that was not affected by the nature of acid. The chitosan blending changed the aggregates interphase and the inner structure of siloxanes domains.

All samples presented fast water uptake with the same initial swelling rate and with a non-Fickian or anomalous transport mechanism. Swelling degree was higher in hybrids prepared with hydrochloric acid, which possessed lower polycondensation degree, while chitosan reduces the hydrophilicity of these OIH.

We can conclude that the chitosan blending on ureasil–PEO hybrid materials provided a means of tailoring the swelling degree of these OIH, which increases their potential use as matrices for controlled drug release.

References

1. Molina EF, Pulcinelli SH, Briois V, Santilli CV. Fine-tuning of a nanostructure, swelling, and drug delivery profile by blending ureasil-PEO and ureasil-PPO hybrids. Polym Chem. 2014;5:1897–904.
2. Lopes L, Molina EF, Chiavacci LA, Santilli CV, Briois V, Pulcinelli SH. Drug–matrix interaction of sodium diclofenac incorporated into ureasil-poly(ethylene oxide) hybrid materials. RSC Adv. 2012;2:5629–36.
3. Molina EF, Parreira RLT, De Faria EH, De Carvalho HWP, Caramori GF, Coimbra DF, et al. Ureasil-poly(ethylene oxide) hybrid matrix for selective adsorption and separation of dyes from water. Langmuir. 2014;30:3857–68.
4. Molina EF, Marçal L, Carvalho HWP, Nassar EJ, Ciuffi KJ. Tri-ureasil gel as a multifunctional organic–inorganic hybrid matrix. Polym Chem. 2013;4:1575–82.
5. Moura ALA, de Oliveira LK, Ciuffi KJ, Molina EF. Influence of the hydrophilic/hydrophobic nature of polyetheramines on the interaction between amine–alcohol–silicate hybrids and anionic dyes for effective water cleaning. J Mater Chem A. 2015;3:16020–32.
6. Paredes Zaldivar M, Pulcinelli SH, Peniche C, Gonçalves V, Santilli CV. Chitosan/(ureasil-PEO hybrid) blend for drug delivery. J Sol-Gel Sci Technol. 2014;72:233–8.
7. Wu N, Wang LS, Tan DCW, Moochhala SM, Yang YY. Mathematical modeling and in vitro study of controlled drug release via a highly swellable and dissoluble polymer matrix: polyethylene oxide with high molecular weights. J Control Release. 2005;102:569–81.
8. Santilli CV, Chiavacci LA, Lopes L, Pulcinelli SH, Oliveira AG. Controlled drug release from ureasil-polyether hybrid materials. Chem Mater. 2009;21:463–7.
9. Croisier F, Jérôme C. Chitosan-based biomaterials for tissue engineering. Eur Polym J. 2013;49:780–92.
10. Laranjeira MCM, Fávere VT. Biopolímero Funcional com Potencial Industrial Biomédico. Quim Nova. 2009;32:672–8.
11. Kim B, La Flamme K, Peppas NA. Dynamic swelling behavior of pH-sensitive anionic hydrogels used for protein delivery. J Appl Polym Sci. 2003;89:1606–13.
12. Ritger PL, Peppas NA. A simple equation for description of solute release II. Fickian and anomalous release from swellable devices. J Control Release. 1987;5:37–42.
13. Serra L, Doménech J, Peppas NA. Drug transport mechanisms and release kinetics from molecularly designed poly(acrylic acid-g-ethylene glycol) hydrogels. Biomaterials. 2006;27:5440–51.
14. Santos JE, Soares JP, Dockal ER, Campana Filho SP, Cavalheiro ÉTG. Caracterização de quitosanas comerciais de diferentes origens. Polímeros. 2003;13:242–9.
15. Wunderlich B. Macromolecular physics. New York: Academic Press; 1980.

16. Ziegler-Borowska M, Chełminiak D, Kaczmarek H. Thermal stability of magnetic nanoparticles coated by blends of modified chitosan and poly(quaternary ammonium) salt. J Therm Anal Calorim. 2014;119:499–506.

17. Barbosa PC, Fernandes M, Vilela SMF, Gonçalves A, Oliveira MC, Fortunato E, et al. Di-ureasil hybrids doped with LiBF4: attractive candidates as electrolytes for "Smart Windows". Int J Electrochem Sci. 2011;6:3355–74.

18. Ziegler-Borowska M, Chelminiak D, Kaczmarek H, Kaczmarek-Kedziera A. Effect of side substituents on thermal stability of the modified chitosan and its nanocomposites with magnetite. J Therm Anal Calorim. 2016;124:1267–80.

19. Pereira FS, Lanfredi S, González ERP, da Silva Agostini DL, Gomes HM, dos Santos Medeiros R. Thermal and morphological study of chitosan metal complexes. J Therm Anal Calorim. 2017;. doi:10.1007/s10973-017-6146-2.

20. Ivanković M, Brnardić I, Ivanković H, Huskić M, Gajović A. Preparation and properties of organic–inorganic hybrids based on poly(methyl methacrylate) and sol–gel polymerized 3-glycidyloxypropyltrimethoxysilane. Polymer. 2009;50:2544–50.

21. Hoebbel D, Nacken M, Schmidt H. A NMR study on the hydrolysis, condensation and epoxide ring-opening reaction in sols and gels of the system glycidoxypropyltrimethoxysilane-water-titaniumtetraethoxide. J Sol-Gel Sci Technol. 1998;12:169–79.

22. Romeo HE, Fanovich MA, Williams RJJ, Matějka L, Pleštil J, Brus J. Self-assembly of a bridged silsesquioxane containing a pendant hydrophobic chain in the organic bridge. Macromolecules. 2007;40:1435–43.

23. Brinker CJ, Scherer GW. Sol–gel science. The physics and chemistry of sol-gel processing. San Diego: Academic Press; 1990.

24. Santilli CV, Sarmento VHV, Dahmouche K, Pulcinelli SH, Craievich AF. Effects of synthesis conditions on the nanostructure of hybrid sols produced by the hydrolytic condensation of (3-methacryloxypropyl)trimethoxysilane. J Phys Chem C. 2009;113:14708–14.

25. Eisenberg P, Erra-Balsells R, Ishikawa Y, Lucas JC, Mauri AN, Nonami H, et al. Cagelike precursors of high-molar-mass silsesquioxanes formed by the hydrolytic condensation of tri-alkoxysilanes. Macromolecules. 2000;33:1940–7.

26. Fasce DP, Williams RJJ, Méchin F, Pascault JP, Llauro MF, Pétiaud R. Synthesis and characterization of polyhedral silsesquioxanes bearing bulky functionalized substituents. Macromolecules. 1999;32:4757–63.

27. Cordes DB, Lickiss PD, Rataboul F. Recent developments in the chemistry of cubic polyhedral oligosilsesquioxanes. Chem Rev. 2010;110:2081–173.

28. Curran MD, Stiegman AE. Morphology and pore structure of silica xerogels made at low pH. J Non Cryst Solids. 1999;249:62–8.

29. Guinier A, Fournet G. Small-angle scattering of X-rays. Progress in crystal growth and characterization. New York: Wiley; 1955.

30. Hammouda B. A new Guinier–Porod model. J Appl Crystallogr. 2010;43:716–9.

31. Peppas NA, Bures P, Leobandung W, Ichikawa H. Hydrogels in pharmaceutical formulations. Eur J Pharm Biopharm. 2000;50:27–46.

32. Chime SA, Onunkwo GC, Onyishi II. Kinetics and mechanisms of drug release from swellable and non swellable matrices: a review. Res J Pharm Biol Chem Sci. 2013;4:97–103.

33. Podual K, Doyle F, Peppas NA. Modeling of water transport in and release from glucose-sensitive swelling-controlled release systems based on poly(diethylaminoethyl methacrylate-g-ethylene glycol). Ind Eng Chem Res. 2004;43:7500–12.